

Catalysis Science & Technology

Accepted Manuscript



This is an *Accepted Manuscript*, which has been through the Royal Society of Chemistry peer review process and has been accepted for publication.

Accepted Manuscripts are published online shortly after acceptance, before technical editing, formatting and proof reading. Using this free service, authors can make their results available to the community, in citable form, before we publish the edited article. We will replace this *Accepted Manuscript* with the edited and formatted *Advance Article* as soon as it is available.

You can find more information about *Accepted Manuscripts* in the [Information for Authors](#).

Please note that technical editing may introduce minor changes to the text and/or graphics, which may alter content. The journal's standard [Terms & Conditions](#) and the [Ethical guidelines](#) still apply. In no event shall the Royal Society of Chemistry be held responsible for any errors or omissions in this *Accepted Manuscript* or any consequences arising from the use of any information it contains.

The Direct Synthesis of Hydrogen Peroxide using Platinum Promoted Gold-Palladium Catalysts

Jennifer K. Edwards^{1*}, James Pritchard¹, Peter J. Miedziak¹, Marco Piccinini¹, Albert F. Carley¹, Qian He², Christopher J. Kiely² and Graham J. Hutchings^{1*}

Cardiff Catalysis Institute, School of Chemistry, Cardiff University, Main Building,
Park Place, Cardiff, CF10 3AT, UK

Department of Materials Science and Engineering, Lehigh University, 5 East Packer
Avenue, Bethlehem, PA 18015-3195, USA

Abstract

The direct synthesis of hydrogen peroxide represents a potentially greener route for the production of this important commodity chemical. It is imperative that high activity catalysts are identified for this reaction that can operate without the need for non-green halide and acid promoters. Supported Au-Pd nano-alloys can be used without the need for such additives and these materials form the basis of this study. We have found that the addition of Pt to TiO₂-supported Au-Pd nano-alloys increases the activity of the catalysts for the direct synthesis of hydrogen peroxide. In addition, when very small amounts of Pt are added, the sequential hydrogenation/decomposition of hydrogen peroxide is suppressed thereby enhancing the selectivity of the process. The catalysts have been analysed by both aberration corrected analytical electron microscopy and X-ray photoelectron spectroscopy.

Introduction

Hydrogen peroxide is a major commodity chemical and at present around 3 million tons per annum are manufactured using an indirect process where the hydrogen and oxygen reactants are not permitted to react directly. This is achieved using substituted anthroquinones as hydrogen carriers.¹ The process is very energy intensive, and the product is concentrated for ease of transport to *ca.* 50-70 vol%. However, most hydrogen peroxide is used at much more dilute levels, closer to 6-8 vol%.² The demand for hydrogen peroxide is increasing, and in 2015 it is anticipated that over 4.3 million tons per annum will be required³. Of particular interest is the use of hydrogen peroxide for the manufacture of propylene oxide by the epoxidation of propene using TS-1 as a catalyst.⁴ The direct synthesis of hydrogen peroxide from hydrogen and oxygen presents a cleaner and more atom efficient alternative route to the current commercial production synthetic procedure of this important commodity chemical.⁵⁻⁷ An obvious challenge in the direct synthesis process is achieving high H₂ selectivity towards H₂O₂ whilst avoiding water formation through over-hydrogenation of H₂O₂. A number of catalysts have been investigated for the direct synthesis of hydrogen peroxide, the vast majority of which are based around Pd.⁷⁻⁹ These catalysts require the addition of acid and halide promoters in the reaction medium to achieve high selectivities at high conversions.^{10, 11} We have previously found that the incorporation of Au into Pd gives a catalyst capable of direct H₂O₂ synthesis with high selectivities in the absence of such non-green stabilisers.¹²⁻¹⁴ However, there is still a need to develop even more active catalyst compositions. In this respect, we propose that beneficial effects could arise from the addition of a small amount of a third metallic component to Au-Pd that might also act as a hydrogenation catalyst. To this end, we have selected Pt for study since it is well known as a component of active

hydrogenation catalysts.¹⁵ The effect of combining Pt with Pd has also been studied previously by Strukul and co-workers,¹⁶ who tested Pd-Pt/ZrO₂-SO₄ and Pd-Au/ZrO₂-SO₄ bimetallic catalysts for the direct synthesis of hydrogen peroxide using acid as a stabiliser. The addition of Pt to Pd was observed to enhance the yield of hydrogen peroxide, but the effect was found to be very sensitive to the amount of Pt added; using a very low Pt content it proved possible to improve the H₂ selectivity from 55 to 70% and enhance subsequent H₂O₂ productivity with respect to the Pd-only catalysts. However, this positive effect on H₂O₂ selectivity was not observed by Lunsford *et al.*,¹⁷ who showed that the addition of 5 at% Pt to a 0.5wt%Pd/SiO₂ catalyst increased the H₂O₂ productivity by a factor of 2.5, but the selectivity of this material was slightly lower than that of the mono-metallic Pd catalyst. This observation may be explained by the presence of halide in the Lunsford studies. They also demonstrated that when the halide was absent from the reaction medium, the Pt-Pd catalysts produced only water from enhanced sequential hydrogenation of hydrogen peroxide. In the current study, we have investigated the addition of Pt to a TiO₂-supported Au-Pd alloy and show that the addition of small amounts of Pt can enhance the activity for the direct synthesis of hydrogen peroxide whilst at the same time suppressing the sequential hydrogenation/decomposition activity, thereby giving a significantly enhanced overall performance.

Experimental

Catalyst preparation

Bimetallic Au-Pd, Pt-Pd and Au-Pt catalysts, and trimetallic Au-Pd-Pt materials were prepared by impregnation of a titania (P25 Degussa) support using aqueous solutions of PdCl₂, HAuCl₄·3H₂O and PtCl₂ (Johnson Matthey) *via* a conventional wet

impregnation technique. For a 2.5 wt% Au-2.5 wt% Pd catalyst the following standard procedure was adopted, with all quantities listed per gram of catalyst. PdCl₂ (0.042 g) was dissolved in a solution of HAuCl₄.3H₂O (5g in 250ml H₂O, 2.5ml) while stirring at 80 °C until the Pd dissolved completely. TiO₂ (P25, Degussa) was then added to the solution and stirred at 80 °C to form a thick paste. The material was dried (110 °C, 16 h) and subsequently calcined in static air (400 °C, 3 h). Monometallic Au and Pd were synthesized using the same protocol. For the synthesis of supported 5 wt% Au-Pd-Pt catalysts an aqueous solution of PtCl₂ (1.0g in 10 ml) was introduced via wet impregnation at the same time as PdCl₂ and HAuCl₄.3H₂O, and corresponding to the intended nominal mono-, bi- or tri-metallic catalyst composition

Direct synthesis of H₂O₂

Caution: These experiments involve high pressures.

The catalysts were evaluated for the direct synthesis of hydrogen peroxide in a stainless steel autoclave (Parr Instruments) with a nominal volume of 100 ml and a maximum working pressure of 14 MPa. The autoclave was equipped with an overhead stirrer (0 – 2000 rpm) and provision for measurement of temperature and pressure. Using the standard reaction conditions we have employed previously,¹¹ the autoclave was charged with the catalyst (0.0100 g), solvent (5.6 g CH₃OH and 2.9 g H₂O), purged three times with 5% H₂/CO₂ (100psi) and then filled with 5% H₂/CO₂ (420psi) and 25% O₂/CO₂ (160psi) to give a hydrogen-to-oxygen ratio of 1 : 2. Stirring (at 1200 rpm) was commenced on reaching the desired temperature (2 °C), and experiments were carried out for 30 min. The H₂O₂ yield was determined by titration of aliquots of the final filtered solution with acidified Ce(SO₄)₂ (7 x 10⁻³ mol l⁻¹). The Ce(SO₄)₂ solutions were standardised against (NH₄)₂Fe(SO₄)₂.6H₂O using

ferroin as an indicator. Each catalyst was tested in triplicate, and the productivity reported an average of the 3 results, the overall accuracy of the experiments is typically $\pm 1 \text{ mol H}_2\text{O}_2 \text{ kg}_{\text{cat}}^{-1} \text{ h}^{-1}$.

Hydrogenation/decomposition of H₂O₂

Hydrogenation experiments were carried in a similar fashion to the synthesis reactions, but with the absence of 25% O₂/CO₂ from the gas stream and in the presence of 4 wt% H₂O₂ in the solvent (solution composition: 5.6 g CH₃OH, 2.22 g H₂O, 0.68 g 50 wt% H₂O₂). The decrease in H₂O₂ concentration (determined from measurements taken before and after reaction) is attributed to the combined effect of the H₂O₂ hydrogenation and H₂O₂ decomposition reactions.

Catalyst characterization

Samples for examination by scanning transmission electron microscopy (STEM) were prepared by dry dispersing the catalyst powder onto a holey carbon film supported by a 300 mesh copper TEM grid. The specimens were then subjected to bright field (BF) and high angle annular dark field (HAADF) - STEM imaging experiments in order to determine particle size distributions and particle morphologies. The instrument used for this analysis was an aberration corrected JEOL 2200 FS (S)TEM operating at 200 kV. This instrument was also equipped with a Noran X-ray energy dispersive spectrometer (XEDS), allowing compositional analysis to be performed on individual metal nanoparticles.

X-Ray Photoelectron Spectroscopy (XPS) analyses were made on a Kratos Axis Ultra DLD spectrometer. Samples were mounted using double-sided adhesive tape, and binding energies were referenced to the C(1s) binding energy of

adventitious carbon contamination that was taken to be 284.7 eV. Monochromatic AlK α radiation was used for all measurements; an analyser pass energy of 160 eV was used for survey scans while 40 eV was employed for detailed regional scans. The intensities of the Au(4f), Pt (4f) and Pd(3d) features were used to derive the Pd/Pt, and Au/Pt surface atom ratios.

Results and Discussion

A systematic series of catalysts comprising bi- and tri-metallic compositions was prepared using the impregnation method, each designed to have a nominal total metal loading of 5 wt%. These materials were evaluated as catalysts for the synthesis and hydrogenation/decomposition of hydrogen peroxide and the results are presented in Table 1. The synthesis activity of the TiO₂-supported Au-Pd and Au-Pt bimetallic catalysts were very similar; however, the hydrogenation activity was decreased when Pd was replaced by Pt (Table 1, entries 1 and 2). It is possible that this effect is due to Pt having a more stable hydride than Pd which may influence the activity. The TiO₂-supported Pd-Pt catalyst was much more active, since the replacement of Au by Pt in the Pd-alloy decreased the hydrogenation/decomposition rate (Table 1, entry 3). It is clear that the incorporation of Pt as a component of the catalyst has a major effect on the catalytic performance. The addition of small amounts of Pt to a TiO₂-supported Au-Pd catalyst, whilst maintaining a constant Au-Pd ratio, has a very marked effect on the catalysis. Initially, the rate of synthesis is enhanced and the rate of hydrogenation/decomposition is decreased (Table 1, entry 4). However, this effect is only observed for the lowest amount of Pt we investigated (*i.e.* 0.05 wt%); at 0.01wt% Pt the synthesis activity was further enhanced, but so was the rate of hydrogenation/decomposition (Table 1, entry 5). Further increasing the concentration

of Pt increased the hydrogenation rate, which correlates to a decrease in the hydrogen peroxide synthesis rates. For comparison, we also investigated a Pd-rich catalyst containing very small amounts of Au and Pt and it is apparent that this catalyst was very active for both the hydrogenation and decomposition reactions (Table 1, entry 8).

Based on the results of our catalysis experiments, it is clear that the addition of a small amount of Pt to Au-Pd alloy catalysts has a marked positive effect on both activity and selectivity. We have very recently reported this type of behaviour for carbon-supported Au-Pd-Pt trimetallic catalysts designed specifically for the selective oxidation of alcohols.¹⁸ It is clear that in the direct H₂O₂ synthesis reaction the optimal effects are observed by the addition of very small amounts of Pt; this is reminiscent of the findings of Strukul and co-workers¹⁶ who investigated bimetallic Pd-Pt catalysts for this reaction.

We next investigated the nanostructure and surface composition of these catalysts using STEM and X-ray photoelectron spectroscopy. We have previously described in some detail the structure of the TiO₂-supported 5 wt% Au-Pd catalysts prepared by impregnation.¹² These Au-Pd alloys often exhibit core-shell structures comprising a Pd-rich shell and a Au-rich core. They also tend to exhibit a bimodal size distribution, with a large population of small Pd-rich nanoparticles together with a small number of much larger Au-rich nanoparticles >20 nm in diameter. We have analysed the corresponding Au-Pt and Pd-Pt bimetallic particles supported on TiO₂. STEM-HAADF images of a Au-Pt/TiO₂ catalyst (Figure 1) reveal a wide particle size distribution, similar to that previously reported for the Au-Pd/TiO₂ system.¹² XEDS analysis of individual particles shows that these nanoparticles are indeed Au-Pt alloys. However, a significant systematic composition variation with particle size was noted, with the larger particles being Au-rich and the smaller ones being enriched in Pt

(Figure 2). The TiO₂-supported Pd-Pt nanoparticles also show a range of particle sizes (Figure 3), along with a distinct systematic composition variation with particle size (Figure 4). In this case, the smaller particles comprise mainly Pd and as the particle size increases, the fraction of Pd in the nanoparticles gradually decreases. For the very smallest particles, a Pt signal was not observed, which means that Pt, if present, is below the detection limit of the XEDS technique.

Representative STEM HAADF micrographs for the 2.4wt%Au-2.4wt%Pd-0.2wt%Pt catalyst are shown in Figure 5. The addition of Pt into the Au-Pd alloy mixture leads to a considerably narrower particle size distribution. XEDS analysis (Figure 6) shows that the smallest particles are very Pd-rich and the amount of Pd in the nano-alloys progressively decreases as the particle size increases. This trend is similar to that observed for Au-Pd bimetallic catalysts prepared by impregnation.⁶ Unfortunately, the Pt content is below the detection limit for the XEDS method and so we cannot comment on whether or not the Pt is uniformly distributed. We also examined the Pd-rich catalyst (0.2wt% Au-4.6wt% Pd-0.2wt% Pt) and found that the material once again comprised very small nanoparticles, but in XEDS analysis only the Pd signal was observed due to the Au and Pt being below the limit of detectability (Figure 7).

XPS analysis of the catalysts was also carried out (Table 2, Figure 8). The experimental Pd/Au atom ratios for the 2.28wt%Au-2.28wt%Pd-0.45wt%Pt and 2.40wt%Au-2.40wt%Pd-0.20wt%Pt trimetallic samples are much higher than those calculated from the nominal compositions, in keeping with the XEDS results which indicate the presence of a large number of small, well-dispersed Pd-rich nanoparticles. The Au(4f) photoemission signal from the less populous, much larger Au-rich particles is attenuated due to the small mean path of the photoelectrons. An alternative

explanation in terms of a Au(core)-Pd(shell) structure is ruled out by the XEDS data, where there is no evidence for a Pd-rich outer layer. The Pd(3d) spectra indicate that the Pd is predominantly present as Pd²⁺ species. For comparison, the Pd/Au molar ratio for the Pt-free Au-Pd/TiO₂ catalyst is 19. For the bimetallic Pd-Pt catalysts, the Pd also dominates the overall surface composition, whereas the Au and Pt signals from the Au-Pt sample are quite similar, which is again in general agreement with the STEM conclusions.

In summary, we have shown that the addition of Pt as a third metallic component to a Au-Pd supported nano-alloy catalyst affects the activity and selectivity in the direct synthesis of hydrogen peroxide. In particular, the addition of a very small amount of Pt can enhance the synthesis whilst suppressing the hydrogenation/decomposition reactions. Pt-doping suppresses the formation of the Pd(shell)-Au(core) particles observed in previous studies¹² of titania-supported bimetallic 2.5wt%Au-2.5wt%Pd catalysts, but leads to well-dispersed small Pd-rich particles. . This study shows that the addition of minor additional components to bimetallic alloy catalysts can be beneficial.

Acknowledgements

We thank Solvay, EPSRC grant [EP/I006060/1](#) and the NSF for financial support. In addition, C.J.K gratefully acknowledges funding from the National Science Foundation Major Research Instrumentation program (GR# MRI/DMR-1040229).

References

1. G. Pfeleiderer and H Rledl, US Patent US2158525, 1939.
2. J. M. Campos-Martin, G. Blanco-Brieva and J. L. G. Fierro, *Angew. Chem., Int., Ed.*, 2006, **45**, 6962-6984.
3. http://www.prweb.com/releases/hydrogen_peroxide/bleaching_pulp_paper/prweb8067430.ht
4. US20100331556A1, 2010.
5. J. K. Edwards, B. Solsona, E. Ntainjua N, A. F. Carley, A. A. Herzing, C. J. Kiely and G. J. Hutchings, *Science*, 2009, **323**, 1037-1041.
6. J. K. Edwards, E. Ntainjua N, A. F. Carley, A. A. Herzing, C. J. Kiely and G. J. Hutchings, *Angew. Chem. Int. Ed.*, 2009, **48**, 8512-8515.
7. V. R. Choudhary and C. Samanta, *Catal. Lett.*, 2005, **99**, 79-81.
8. J. H. Lunsford, *J. Catal.*, 2003, **216**, 455-460.
9. V. R. Choudhary, A. G. Gaikwad and S. D. Sansare, *Catal. Lett.*, 2002, **83**, 235-239.
10. V. R. Choudhary and P. Jana, *App. Cat. A. Gen.*, 2009, **352**, 35-42.
11. V. R. Choudhary and P. Jana, *App. Cat. A. Gen.*, 2007, **329**, 79-85.
12. J. K. Edwards, B. E. Solsona, P. Landon, A. F. Carley, A. Herzing, C. J. Kiely and G. J. Hutchings, *J. Catal.*, 2005, **236**, 69-79.
13. J. K. Edwards, A. Thomas, A. F. Carley, A. A. Herzing, C. J. Kiely and G. J. Hutchings, *Green Chem.*, 2008, **10**, 388-394.
14. J. K. Edwards, A. Thomas, B. E. Solsona, P. Landon, A. F. Carley and G. J. Hutchings, *Catal. Today*, 2007, **122**, 397-402.
15. S. D. Lin and M. A. Vannice, *J. Catal.*, 1993, **143**, 539-553.
16. G. Bernardotto, F. Menegazzo, F. Pinna, M. Signoretto, G. Cruciani and G. Strukul, *App. Cat. A. Gen.*, 2009, **358**, 129-135.
17. Q. Liu, J. C. Bauer, R. E. Schaak and J. H. Lunsford, *App. Cat. A. Gen.*, 2008, **339**, 130-136.
18. Q. He, P. J. Miedziak, L. Kesavan, N. Dimitratos, M. Sankar, J. A. Lopez-Sanchez, M. M. Forde, J. K. Edwards, D. W. Knight, S. H. Taylor, C. J. Kiely and G. J. Hutchings, *Farad. Discuss.*, 2013, **162**, 365-378.

Table 1 Effect of addition of Pt to Au-Pd nanoparticles supported on TiO₂ for the direct H₂O₂ reaction.

| Entry | Composition / wt% | Productivity | Hydrogenation |
|-------|---|---|---|
| | | mol _{H₂O₂} kg _{cat} ⁻¹ h ⁻¹ | mol _{H₂O₂} kg _{cat} ⁻¹ h ⁻¹ |
| 1 | 2.50% Au-2.50% Pd ^a | 64 | 235 |
| 2 | 2.50% Au-2.50% Pt ^b | 65 | 103 |
| 3 | 2.50% Pd-2.50% Pt ^c | 124 | 129 |
| 4 | 2.45% Au-2.45% Pd-0.05% Pt ^d | 154 | 135 |
| 5 | 2.45% Au-2.45% Pd-0.10% Pt ^e | 159 | 283 |
| 6 | 2.40% Au-2.40% Pd-0.20% Pt ^f | 156 | 318 |
| 7 | 2.28% Au-2.28% Pd-0.45% Pt ^g | 106 | 263 |
| 8 | 0.20% Au-4.60% Pd-0.20% Pt ^h | 184 | 382 |

^a 1:1.9 mol% Au: Pd, ^b 1:1 mol% Au: Pt, ^c 1.9:1 mol% Pd: Pt, ^d 1:1.9:0.025 mol% Au: Pd: Pt, ^e 1:1.9:0.05 mol% Au: Pd: Pt, ^f 1:1.9:0.1 mol% Au: Pd: Pt, ^g 1:1.9:0.2 mol% Au: Pd: Pt, ^h 1:43:1

Table 2 Summary of the XPS-derived surface atomic concentrations for binary Au-Pt, Pd-Pt and trimetallic Au-Pd-Pt catalysts supported on TiO₂.

| TiO ₂ support Composition / wt% | Surface atom % | | | |
|---|----------------|------|-------|-------|
| | Au | Pd | Pt | Pd/Au |
| 2.28% Au-2.28% Pd-0.45% Pt | 0.06 | 2.00 | 0.17 | 36** |
| 2.40% Au-2.40% Pd-0.20% Pt | 0.16 | 2.09 | 0.00* | 13** |
| 0.20% Au-4.60% Pd-0.20% Pt | 0.00* | 4.45 | 0.10 | - |
| 2.50% Pd-2.50% Pt | 0.0 | 1.23 | 0.27 | |
| 2.50% Au-2.50% Pt | 0.22 | 0.0 | 0.31 | |

*Below detection limits

**Expected value 1.9

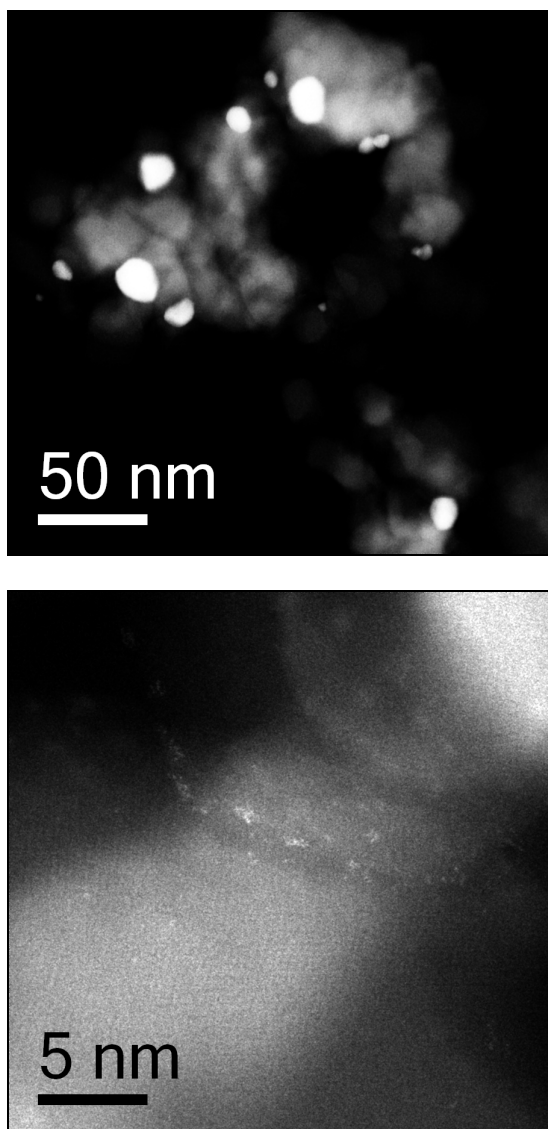
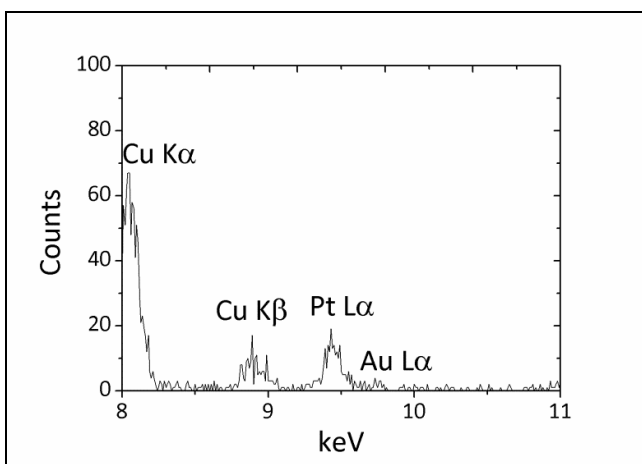
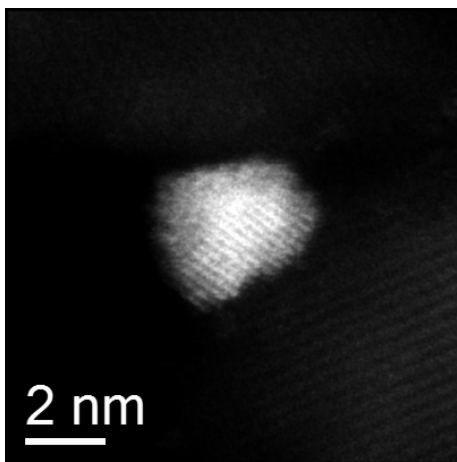
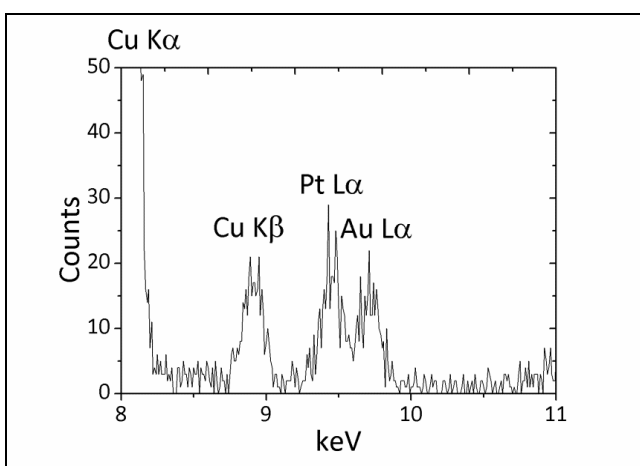
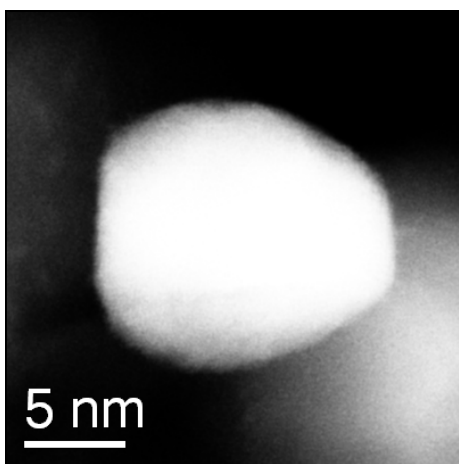


Figure 1 Representative STEM-HAADF images of the 2.50 wt% Au-2.50 wt% Pt/TiO₂ bimetallic catalyst. The low magnification micrograph (*left*) shows the presence of large nanoparticles *ca* 20 nm in diameter, whereas the higher magnification micrograph (*right*) shows that sub-nm clusters are also present.





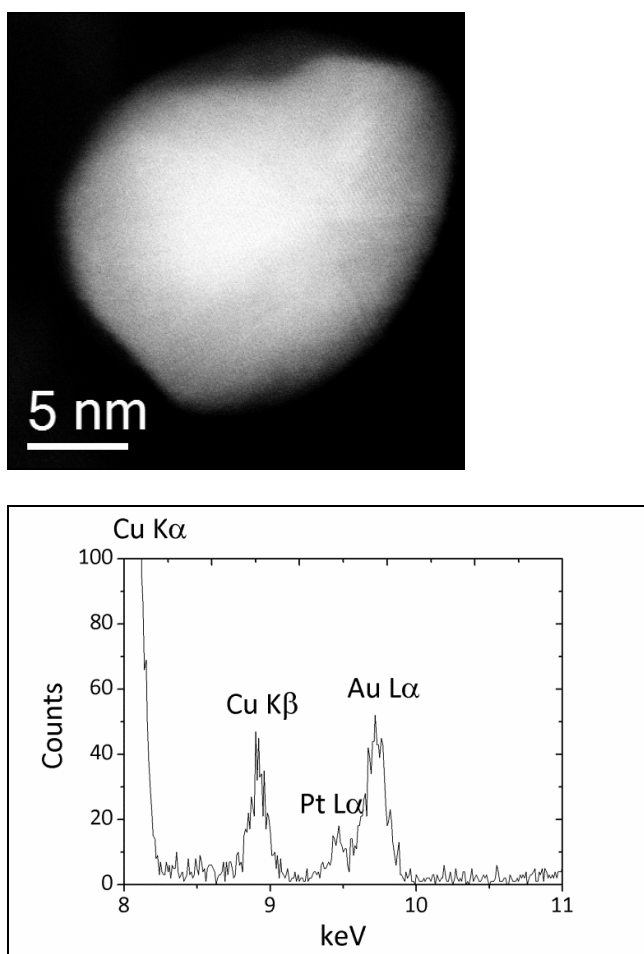


Figure 2 STEM-XEDS analyses of the 2.50 wt% Au-2.50 wt% Pt/TiO₂ bimetallic catalyst, showing the typical composition of small (*top*), intermediate (*middle*) and large (*bottom*) size Au-Pt particles. A systematic composition /size variation was noted with the larger particles being Au-rich and the smaller ones being Pt-rich. Note the presence of Cu signal(s) in the XEDS spectra which represent an artefact from the support grid and are not characteristic of the catalyst samples.

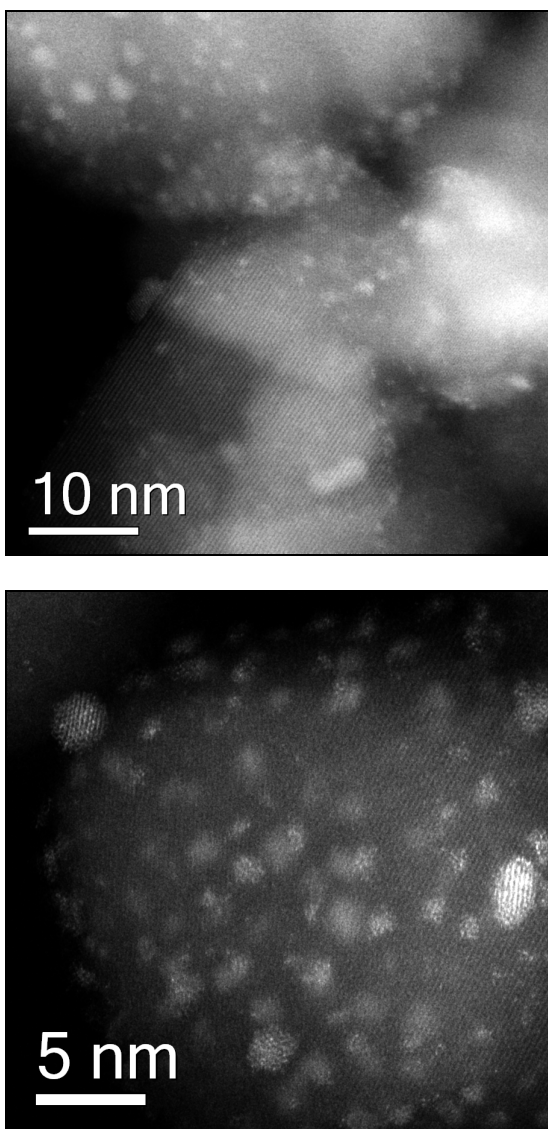
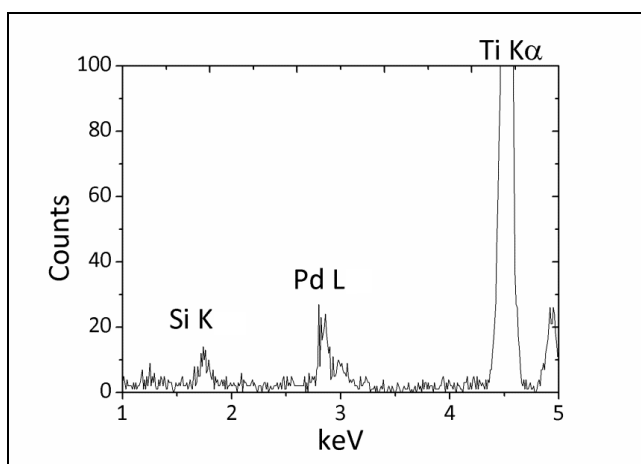
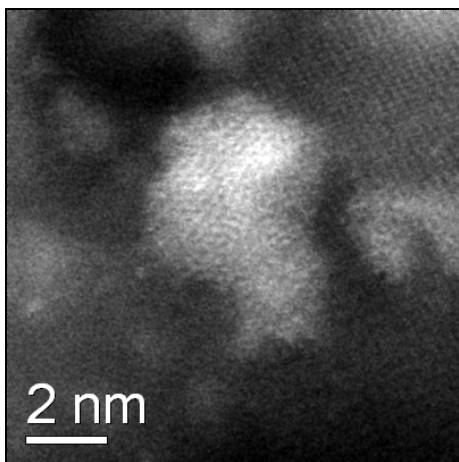
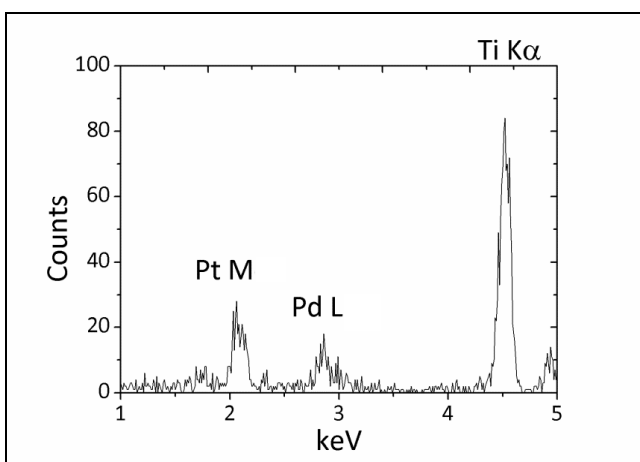
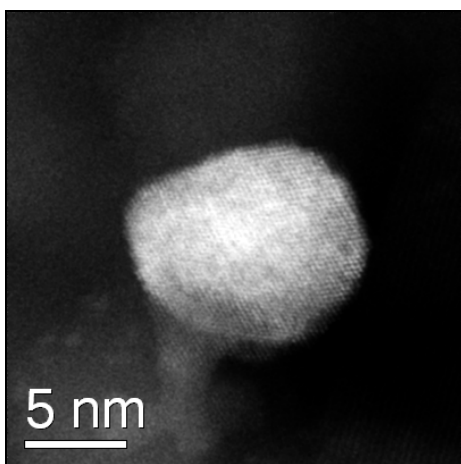


Figure 3 Representative low (*left*) and high (*right*) magnification STEM-HAADF images of the 2.50 wt% Pd-2.50 wt% Pt/TiO₂ bimetallic catalyst.





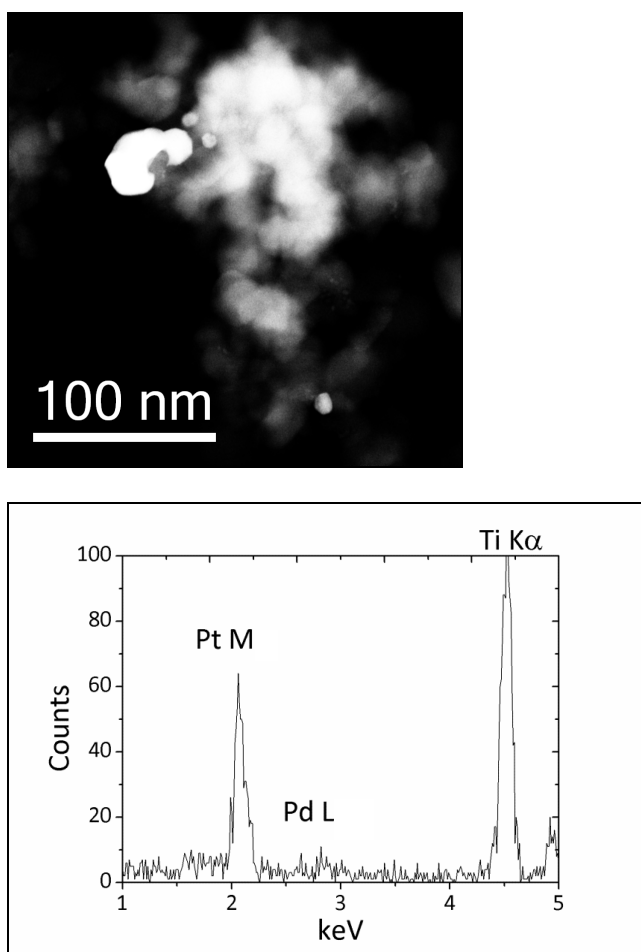


Figure 4 STEM-XEDS analyses of the 2.50 wt% Pd-2.50 wt% Pt/TiO₂ bimetallic catalyst, showing the typical compositions of small (*top*), intermediate (*middle*) and large (*bottom*) size Pd-Pt particles. A systematic composition /size variation was noted with the larger particles being Pt-rich and the smaller ones being Pd-rich.

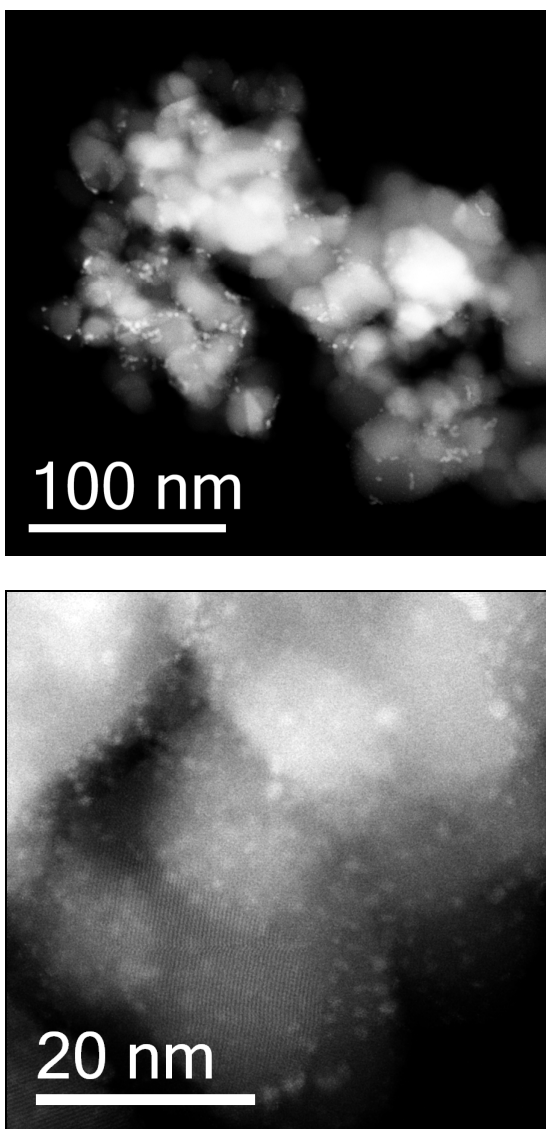
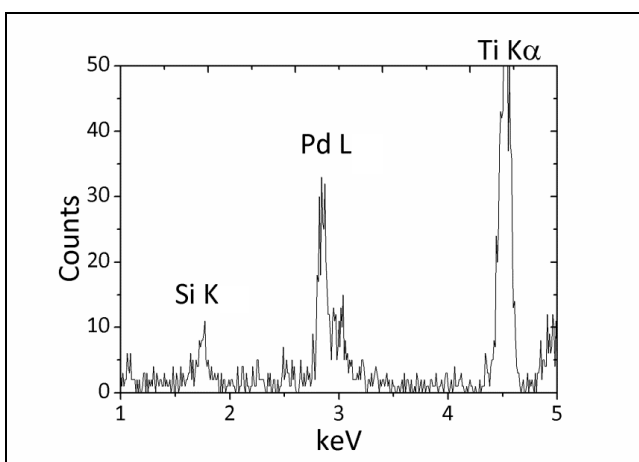
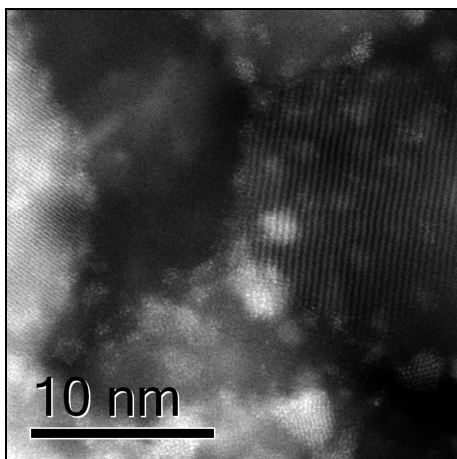


Figure 5 Representative low (*left*) and high (*right*) magnification STEM-HAADF images of the 2.40 wt% Au-2.40 wt% Pd-0.20 wt% Pt/TiO₂ trimetallic catalyst.



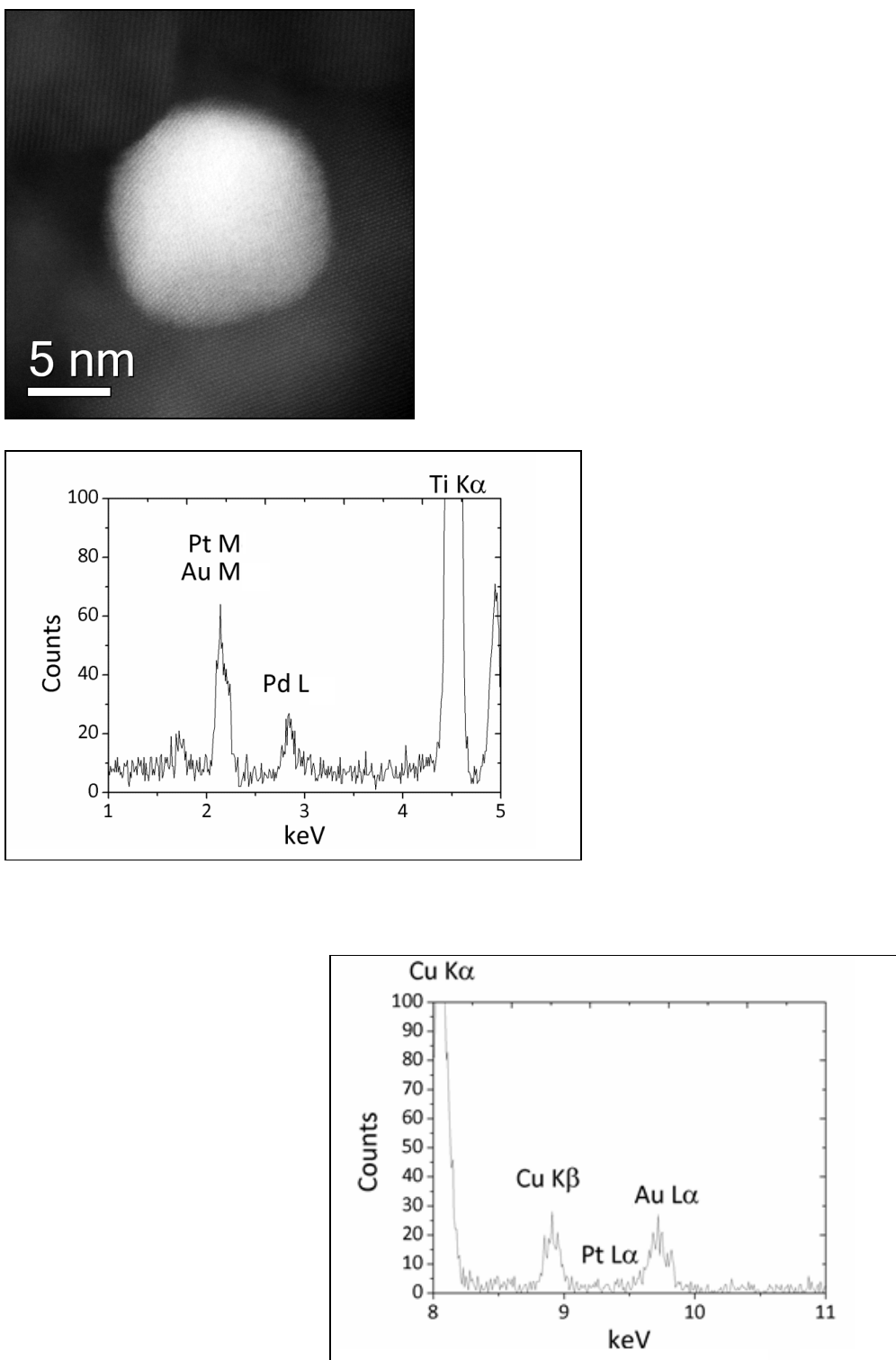
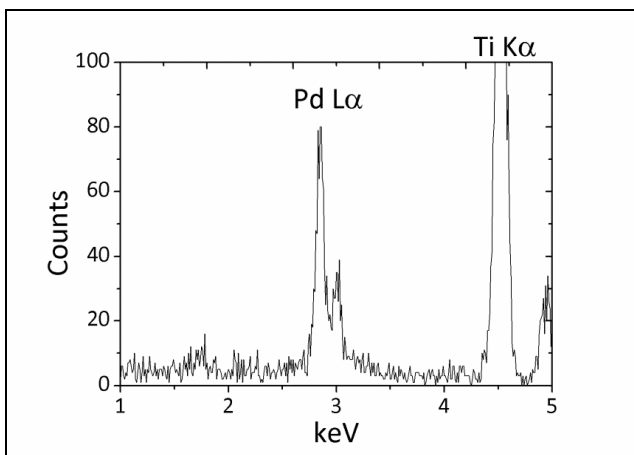
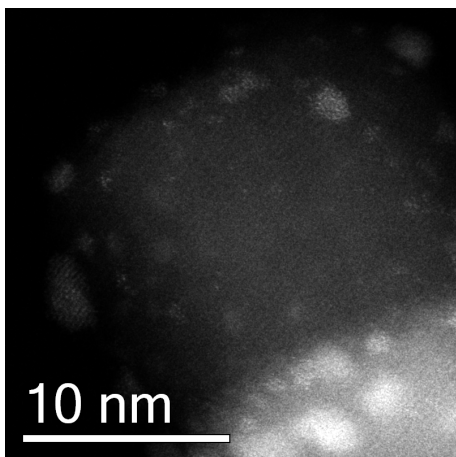


Figure 6 STEM-EDS analyses of the 2.40 wt% Au-2.40 wt% Pd-0.20 wt% Pt/TiO₂ trimetallic catalyst showing the typical compositions of smaller (*top*) and larger

(*bottom*) size Au-Pd-Pt particles (Note;-the two lower spectra obtained from the same particle cover different spectral regions and display the Pt/Au M, Pd L peaks and Pt L, Au L peaks respectively).



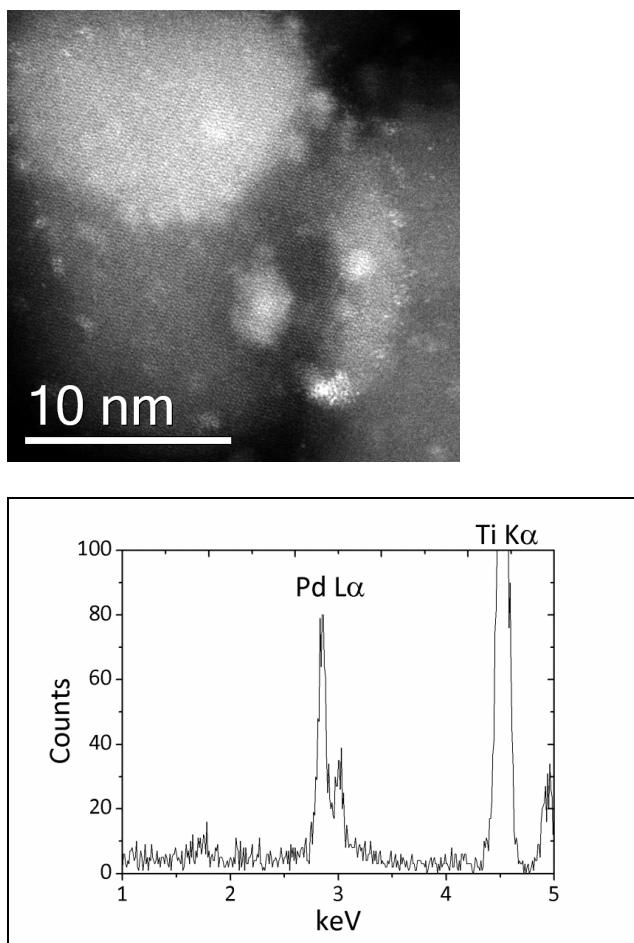


Figure 7 Representative STEM-HAADF images of 0.20 wt% Au-4.60 wt% Pd-0.20 wt% Pt/TiO₂ trimetallic catalyst and the corresponding XEDS spectra obtained from these regions.

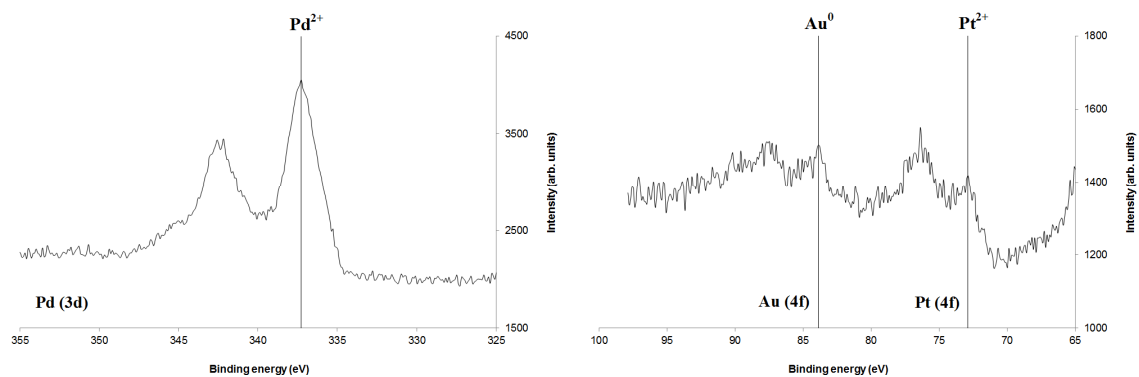


Figure 8 Pd (3d) XPS spectrum (*left*), and Au (4f) and Pt (4f) XPS spectra (*right*) obtained from the 2.28 wt% Au-2.28 wt% Pd-0.45 wt% Pt/TiO₂ trimetallic catalyst.